A Ka-band CMOS Active Phase Shifter Using Active Balun for Phase Optimization

Jimin Lee[1], Jaeyong Lee[2], Seongjin Jang[3], Changkun Park[4]

Intelligent Microwave System. Lab, Soongsil University, Republic of Korea

{[1]jiminny2, [2]mirinae38, [3]jsj0613}@soongsil.ac.kr, [4]pck77@ssu.ac.kr

***Abstract* — In this paper, we designed a CMOS active phase shifter that operates in the Ka-band. In the active phase shifter, the differential signals with high phase accuracy were generated using active balun to alleviate complexity, thereby reducing the insertion loss of I/Q generator. In addition, we proposed a layout technique that can secure symmetry between the output signals of poly phase filter (PPF). To verify the feasibility of the proposed design technique, we designed an Ka-band active phase shifter using 65 nm RFCMOS process. The core size of the designed phase shifter was 0.506 × 0.257 mm². At the target frequency of 28 GHz, the measured RMS phase and gain errors were lower than 0.35° and 0.07 dB, respectively.**

***Keywords* — Active balun, mm-wave, phased array, phase resolution, phase shifter.**

I. Introduction

With the continuous development of wireless communication technology, 5G wireless communication technology using the millimetre wave (mmWave) band is being actively studied. In the 5G communication, beamforming technology through the array antenna system is continuously being studied. Since beamforming is a technology that focuses signals in a specific direction by controlling the phases and amplitudes of the several antenna patterns constituting the array antenna, the phase shifter that controls the phase of the output signal is one of the key circuits in 5G communication [1], [2].

In general, phase shifter has two types; passive and active types. Although the passive phase shifter allows bidirectional signal flow, there are problems such as the bulky size and relatively high power loss [3]. On the other hand, active phase shifters have advantages of generating gains to compensate for insertion losses, providing higher phase resolutions compared to passive phase shifters, and having a compact size [4]. However, given than as shown in Fig. 1, the active phase shifter consisting of input balun, I/Q generator, and Gilbert cells, the I/Q generator may also cause signal loss. Therefore, the amplification stage of the active phase shifter is required to alleviate the signal loss. In this work, the I/Q generator was designed with poly-phase filter (PPF).

In this study, to mitigate the signal loss, the required number of PPF units was reduced by increasing the accuracy of the 180° phase of the balun output signal. To this end, an active balun was proposed. We also proposed a layout technique that can improve the symmetry between the output signals of PPF.

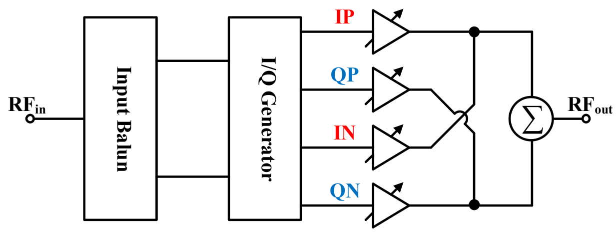

Fig. 1. Block –diagram of the active phase shifter

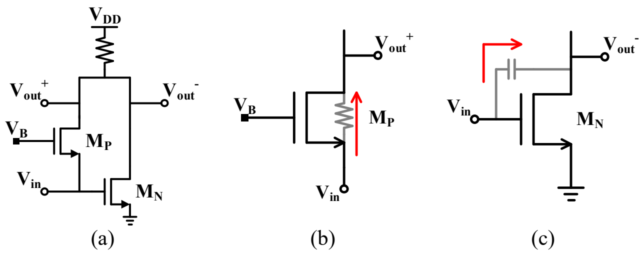

Fig. 2. Conventional active balun (a) CS-CG structure active balun, (b) output variation of CG and (c) output variation of CS.

II. Design of the Proposed Active Phase Shifter

Active phase shifter is a circuit that controls the desired phase and gain by vector summing four orthogonal quadrature signals. Input balun and I/Q generator generate quadrature signals. In general, differential signals were generated through transformers or couplers, and I/Q signals were finally generated through the I/Q generator of the filter structure. This structure results in high insertion loss, which degrades the performance of the phase shifter.

Differential signals generated through passive balun such as transformers and couplers have large insertion loss in high frequency bands, and it is difficult to obtain high accuracy of 180° phase between differential signals. This phase imbalance of the differential signal affects the output of the I/Q generator, causing a phase variation. As a result, the I/Q generator becomes complex in structure to remove phase variation of the passive balun, so the insertion loss becomes increased.

In this study, to solve the problem of loss of input balun and alleviate the phase imbalance of differential signals, we used active balun to generate differential signals with gains and optimize the output phase difference. We also propose an improved RC PPF structure to simplify the I/Q generator structure to reduce insertion loss, thereby improving the performance of the active phase shifter.

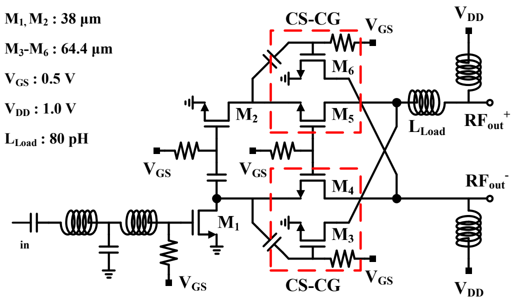

Fig. 3. Schematic of proposed active balun.

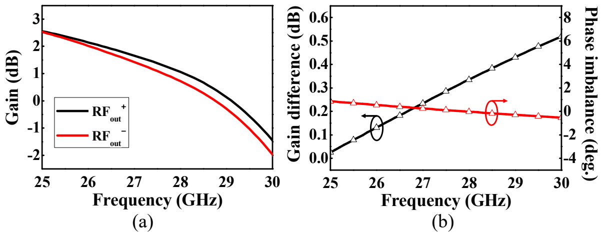

Fig. 4. Simulation result of proposed active balun (a) output gain, (b) phase imbalance and gain difference.

A. *Active Balun*

Fig. 2 (a) shows a conventional active balun with common-source (CS) and common-gate (CG) amplifiers. This structure generates a differential signal using the inverted output phase of the CS amplifier and the non-inverted output phase of the CG amplifier. However, because the frequency is high in the mmWave region, the parasitic component of the transistor affects the phase of the output signal. Fig. 2 (b) shows the input signal passing through R_{ON} of M_P in the CG amplifier and Fig. 2 (c) shows the input signal passing through C_{gd} of M_N in the CS amplifier. The generated differential signals pass through different paths and are influenced by parasitic components, resulting in gain and phase errors. Other active baluns are also affected by the parasitic component of the transistor, making it difficult to generate a complete differential signals.

To solve this problem, the active balun as shown in Fig. 3 is proposed. The proposed active balun consists of CS and CG cascade structures and phase correction technique (PCT) circuit. The PCT circuit compensates phase and gain errors that generated when a differential signal is initially generated [5]. The proposed active balun, which has two CS-CG pairs, corrects the output phase and gain by vector summing the output signals. In addition, to minimize the gain and phase imbalances, an inductor with an 80 pH was used at one side of the output port of the active balun.

Fig. 4 is a simulation results of the designed active balun. As shown in Fig. 4 (b), at the target frequency of 28 GHz, the output differential signal has a phase imbalance of 0.029° and a gain difference of 0.3 dB. In the frequency range of 26 GHz to 30 GHz, the phase imbalance was lower than 1.5° and the gain difference was lower than 0.52 dB

B. *Single-stage RC poly Phase Filter*

RC PPF is an I/Q generator having a filter structure consisting of a resistor and a capacitor. The structure of the RC

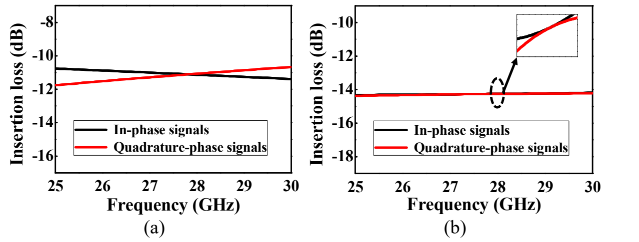

Fig. 5. Insertion loss of RC PPF (a) single-stage RC PPF and (b) double-stage RC PPF.

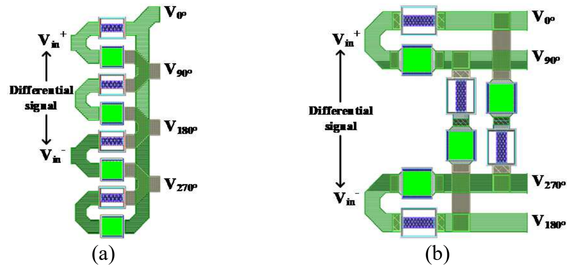

Fig. 6. Layout of RC PPF (a) asymmetry model and (b) proposed symmetry model.

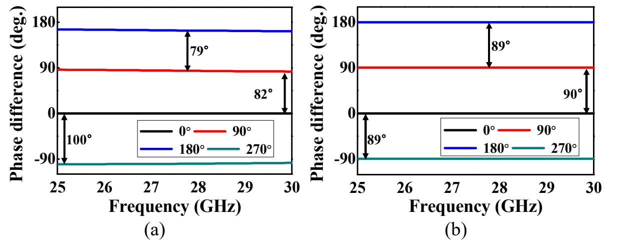

Fig. 7. Phase difference of RC PPF with EM simulation (a) asymmetry RC PPF and (b) symmetry RC PPF.

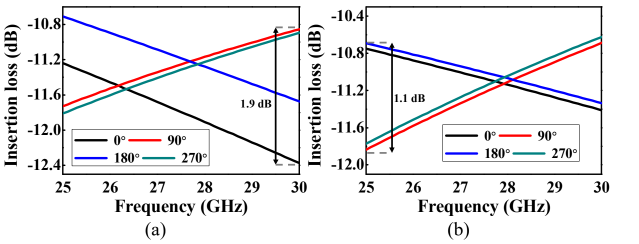

Fig. 8. Insertion loss of RC PPF with EM simulation (a) asymmetry RC PPF and (b) symmetry RC PPF.

PPF is simple, but if the phase difference of the input differential signal is unstable, a phase error of the output I/Q signal occurs. In addition, if the RC PPF has an asymmetric structure, the asymmetry causes additional impedance imbalance to deteriorate the performance of the active phase shifter. To solve this problem, the symmetric structure is repeatedly placed. As a result, the complexity of the circuit increases and the loss increases.

Fig. 5 shows the insertion loss of 1- and 2-stage RC PPFs at the schematic level. As can be seen in Fig. 5, the insertion loss increases as the structure is repeatedly-arranged. Therefore, it is necessary to reduce the number of stages of RC PPF to reduce loss. Since the differential output signals generated by the proposed active balun has a relatively stable phase difference, it is possible to design a single-stage RC PPF as an I/Q

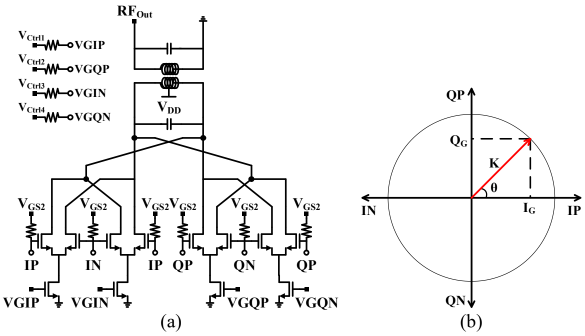

Fig. 9. (a) Schematic of Gilbert cell, output transformer and (b) vector sum theorem.

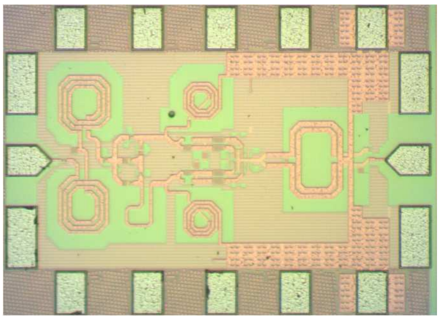

Fig. 10. Photograph of the designed active phase shifter.

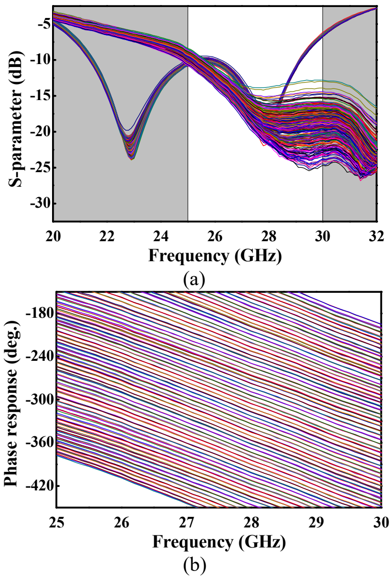

Fig. 11. Measurement results of active phase shifter (a) S-parameter and (b) output phase response.

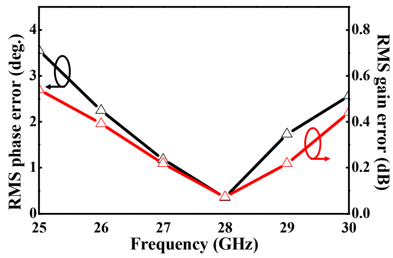

Fig. 12. RMS phase error and gain error

generator, which reduces the insertion loss of the I/Q generator and reduces complexity.

In addition, Fig. 6 (a) shows that the signal line length of the RC PPF are different from each other. The difference causes the impedance imbalance to generate a phase error, which decreases the performance of the I/Q generator. We propose the symmetrical layout technique of Fig. 6 (b) to solve the problem of typical RC PPF. Fig. 7 shows the insertion loss of proposed RC PPF and asymmetric RC PPF reflecting EM simulation. Through this, the proposed RC PPF structure confirmed that the magnitude imbalance was improved by 0.8 dB. Fig. 8 shows that the proposed RC PPF generates a more accurate 90 degree phase difference than the asymmetry RC PPF. Therefore, the proposed RC PPF can eliminate phase variations in the I/Q generator and reduce the performance degradation of the active phase shifter.

C. Gilbert cell, Output transformer

The I/Q signals output through the I/Q generator are orthogonal to each other. Active phase shifter uses vector summation for these I/Q signals to control output phase and gain. To implement the vector sum, four independent current sources for the variable gain amplifier (VGA) function were added to the Gilbert cell mixer as shown in Fig. 9 (a). Gilbert cell is a dual-equilibrium mixer structure that can be less affected by other circuits in an integrated circuit by synthesizing desired signals and suppressing unwanted signals, through on/off.

Designed Gilbert cell determines the gain by adjusting the current source value through voltage variation, and controls the phase and gain by selectively amplifying and synthesizing I/Q signals. After that, it is finally synthesized and output through output transformer. The output value is expressed as a vector sum as shown in Fig. 9 (b). The gain is

$$K = \sqrt{{I_G}^2 + {Q_G}^2} \tag{1}$$

and the phase is

$$\theta = tan^{-1}\left(\frac{Q_G}{I_G}\right). \tag{2}$$

The CS stage and current source of the Gilbert cell were designed using the transistor size of 42 μm and 96 μm, respectively.

III. MEASUREMENTS OF DESIGNED CIRCUIT

The designed active phase shifter was designed using a 65-nm RFCMOS process, the f_t and f_{max} of transistor used in this circuit are 203.9 GHz and 124.6 GHz or higher. To confirm this, V_{GS} and V_{DS} were supplied with 0.5 V and 1 V for the transistor size used. Fig. 10 shows the chip photograph of the designed circuit. The size including the pad is 0.690 × 0.500 mm^2 and the core size is 0.506 × 0.257 mm^2. The gate bias of the active balun and Gilbert cell used 0.5 V and 0.7 V, respectively. The supply voltage used 1.0 V for both active balun and Gilbert cells. The current sources of the Gilbert cell control currents by the control voltages of four pairs of Gilbert cells: (VGIP, VGQP), (VGIN, VGQP), (VGIN, VGQP), and (VGIP, VGQN). Each control voltage is supplied with a voltage between 0 and 0.8 V. The current source is turned off by setting the gate voltage to 0 V.

Table 1. Comparison table of the recently published 5G mm-wave Si-based active phase shifter.

Reference	[6]EUMC'18	[7]TCSII'21	[8]MWCL'18	[9]ESSCIRC'22	[10]ICMMT'21	This work
CMOS Tech. (nm)	65	65	180	65	40	65
Topology	Vector Sum	Multi-Vector Sum	Vector Sum	Passive VSPS	Vector Sum	Vector Sum
Frequency (GHz)	27.4-28.6	30.0-32.5	27-33	26.5-29.5	19.7-23.2	25-30
Phase range (°) / Phase resolution (°)	360 / 5.625	360 / 22.5	360 / cont.	360 / 11.25	360 / 5.625	360/cont.
RMS phase error (°)	<0.54	2.2-3.5	0.51-4	<1.77	<1.1	0.35-3.55
RMS gain error (dB)	<0.13	<0.4	0.86-1.3	<0.27	<0.19	0.07-0.54
P_{DC} (mW)	25.2	18	6.6	0	36	38**
Core area (mm^2)	0.32	0.21	0.31	0.1	0.485*	0.13

*Chip Size, **Quiescent current.

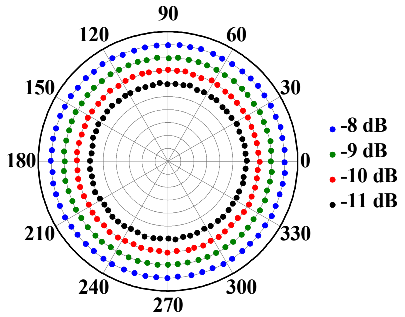

Fig. 13. Measured static constellation diagram of the active phase shifter at 28 GHz.

In this study, at the target frequency of 28 GHz, measurements were conducted in a phase resolution of 5.625° and a gain range of -11 to -8 dB for clarity of the results, and gain control was conducted in 1 dB. In addition, except for the target frequency, the reference for RMS phase error and RMS gain error was based on 0 degree states.

Fig. 11 is the measured value of active phase shifter. As shown in Fig. 11 (a), S_{11} and S_{22} are values corresponding to 0 degree states for each gain. S_{11} is less than -6.18 dB and S_{22} is less than -8.37 dB in the target frequency band. Fig. 11 (b) is phase response and Fig. 12 shows the measured RMS errors. Within the target frequency band, RMS phase and RMS gain errors were lower than 3.55° and 0.54 dB, and at the target frequency of 28 GHz, RMS phase and gain error were 0.35° and 0.07 dB, respectively. RMS phase error was obtained through

$$\sqrt{\frac{1}{n-1}\sum_{k=0}^{n}(\theta_k-\theta_i)^2} \tag{3}$$

where θ_k represents the measured value and θ_i is the reference. RMS gain error was obtained through

$$\sqrt{\frac{1}{n-1}\sum_{k=0}^{n}(G_k-G_i)^2} \tag{4}$$

where G_k is the measurement value and G_i is the reference. Fig.13 is the measured constellation diagram with gain and phase states.

IV. Conclusion

In this study, we designed an active phase shifter using the 65-nm RFCMOS process. The phase shifter consists of active balun, single-stage RC PPF, Gilbert cell, and output transformer. By using active balun, a differential signal with gain in the high frequency band was generated, and single-stage RC PPF was used by optimizing the output phase difference of the output differential signal. We also propose a symmetrical layout technique of the RC PPF to solve the phase variation due to the asymmetric structure of typical RC PPF. In frequency range from 25 to 30 GHz, RMS phase error and RMS gain error are 3.55° and 0.54 dB, S_{11}, S_{22} are lower than -6.18 dB and -8.37 dB.

Acknowledgment

This work was supported in part by the National Research Foundation of Korea (NRF) grant funded by the Korea government (MSIT) (No. 2021R1A2C1013666) and in part by the National Research Foundation of Korea (NRF) through the Korea Government (MSIT) under Grant NRF-2021R1A4A1032580.

References

[1] B. -W. Min and G. M. Rebeiz, "Single-Ended and Differential Ka-Band BiCMOS Phased Array Front-Ends," *IEEE Journal of Solid-State Circuits*, vol. 43, no. 10, pp. 2239-2250, Oct. 2008.

[2] M. Tabesh et al., "A 65 nm CMOS 4-Element Sub-34 mW/Element 60 GHz Phased-Array Transceiver," *IEEE Journal of Solid-State Circuits*, vol. 46, no. 12, pp. 3018-3032, Dec. 2011.

[3] G. -S. Shin et al., "Low Insertion Loss, Compact 4-bit Phase Shifter in 65 nm CMOS for 5G Applications," *IEEE Microwave and Wireless Components Letters*, vol. 26, no. 1, pp. 37-39, Jan. 2016.

[4] K. -J. Koh and G. M. Rebeiz, "0.13-µm CMOS Phase Shifters for X-, Ku-, and K-Band Phased Arrays," *IEEE Journal of Solid-State Circuits*, vol. 42, no. 11, pp. 2535-2546, Nov. 2007.

[5] H. Chiang, F. Huang, C. Wang and C. Wang, "A 90 nm CMOS V-Band Low-Noise Active Balun With Broadband Phase-Correction Technique," *IEEE J. Solid-State Circuits*, vol. 46, no. 11, pp. 2583-2591, Nov. 2011.

[6] J. Pang, R. Kubozoe, Z. Li, M. Kawabuchi and K. Okada, "A 28GHz CMOS Phase Shifter Supporting 11.2Gb/s in 256QAM with an RMS Gain Error of 0.13dB for 5G Mobile Network," in *2018 48th European Microwave Conference (EuMC)*, 2018, pp. 807-810.

[7] J. Park, G. Jeong and S. Hong, "A Ka-Band Variable-Gain Phase Shifter With Multiple Vector Generators," *IEEE Trans. Circuits Syst. II: Express Briefs*, vol. 68, no. 6, pp. 1798-1802, June 2021.

[8] Y. -T. Chang, Z. -W. Ou, H. Alsuraisry, A. Sayed and H. -C. Lu, "A 28-GHz Low-Power Vector-Sum Phase Shifter Using Biphase Modulator and Current Reused Technique," *IEEE Microw. Wireless Compon. Lett.*, vol. 28, no. 11, pp. 1014-1016, Nov.

[9] M. Tang, Y. Zhang, J. Pang, A. Shirane and K. Okada, "A 28GHz Area-Efficient CMOS Vector-Summing Phase Shifter Utilizing Phase-Inverting Type-I Poly-Phase Filter for 5G New Radio," in *ESSCIRC 2022- IEEE 48th European Solid State Circuits Conference (ESSCIRC)*, 2022, pp. 333-336.

[10] M. Hu, Q. Li and L. Xu, "A Ka-band 6-bit Digital Active Phase Shifter with High Accuracy in 40nm CMOS Technology," in *2021 International Conference on Microwave and Millimeter Wave Technology (ICMMT)*, 2021, pp. 1-3.